Asynchronous Localization with Mobility Prediction for Underwater Acoustic Sensor Network

Jing Yan, Xiaoning Zhang, Xiaoyuan Luo, Yiyin Wang, Cailian Chen, and Xinping Guan

***Abstract*—For underwater acoustic sensor networks (UASNs), localization of sensor nodes is one of the most important task. However, the harsh aqueous environment such as asynchronous clock and mobile nodes makes underwater localization a challenging problem. In this paper, we present a mobility-based asynchronous localization algorithm for UASNs. Different from the general sensor network, a hybrid architecture including AUVs, active and passive sensor nodes is designed, where AUVs act as anchor nodes to provide localization information for sensor nodes. To eliminate the effect of asynchronous clock and compensate the mobility of sensor nodes, an asynchronous localization algorithm with mobility prediction is provided to obtain the locations of sensor nodes. To solve the localization optimization problem, iterative least square estimators are designed, where Cramer-Rao lower bound and error analysis are also given. Finally, simulation results show that the proposed localization approach can be reduce the localization time by compared with the exhaustive search-based localization method. Meanwhile, the asynchronous algorithm in this paper can effectively eliminate the impact of the clock asynchronization.**

***Index Terms*—Localization; Asynchronous; Mobility; Underwater Acoustic Sensor Networks; AUV**

I. Introduction

In recent years, underwater acoustic sensor networks (UASNs) have been proposed to explore the ocean and support solutions for time-critical aquatic applications, such as port surveillance, environment monitoring, diaster prevention and mine reconnaissance, see [1], [2] and references therein. For UASNs, localization of sensor nodes is one of the most important task, and this critical importance arises from its role in fundamental operations. For instance, monitoring applications often require the location of sensor nodes to get location-aware data. Additionally, most geographic routing protocols assume the availability of location information [3].

Generally speaking, localization schemes for wireless sensor networks can be classified into two types: range-based schemes and range-free schemes (see [4], [5] and references therein). Range-based schemes rely on various mechanisms such as time of arrival (TOA), time difference of arrivals (TDOA), angle of arrival (AOA), or received signal strength indicator (RSSI) to measure the distances and then convert these distance measurements to position information. These kinds of scheme have a higher accuracy, but they need additional hardware for distance measures, which can increase the network cost. On the other hand, the range-free schemes do not need distance measurements, but can only provide coarse localization information. Alternatively, we are more interested in designing a range-based approach to acquire the accurate localization of underwater sensor nodes. However, due to the unique characteristics of UASNs, the issue of how to apply these schemes to UASNs is not well studied.

Compared with the general localization problem, underwater localization has some fundamental differences. Firstly, due to the strong attenuation of electromagnetic waves in water, the global positioning system (GPS) technology is unavailable in an underwater environment. Although some methods have been proposed to achieve the underwater localization such as the inertial measurement unit [6] and Doppler Velocity Log [7], these methods suffer from the error accumulation problem. Subsequently, the propagation delay in underwater environment is five orders of magnitude higher than in radio frequency (RF) terrestrial channels. With the TOA or TDOA, some timing-based approaches are proposed to determine distances between sensor nodes, such as long-baseline (LBL) and short-baseline (SBL) methods as well as their many improvements [8], [9], [10], [11]. Nevertheless, these localization algorithms rely on the clock synchronization assumption, i.e., the clocks for transmitter and receiver are assumed to be synchronized. Since the high propagation delay can cause synchronization errors (i.e., the clocks for sensor nodes are asynchronous), it is not easy to apply these algorithms to the UASNs. Inspired by this, two asynchronous localization algorithms were proposed in [12], [13], however the sensor nodes are assumed to be static and they only work in static underwater environment.

For underwater localization, mobility is an important factor that must be considered, as the sensor nodes often have passive mobility caused by water current or tides [14]. In such a situation, it is difficult to estimate the real distance between two nodes, which in turn leads to the decrease of localization accuracy. In [15], a meandering current mobility model was presented to describe the movement of sensor nodes, where the effect of meandering sub-surface currents and vortices are both considered. Based on the above mobility model, some mobility prediction strategies were applied to the underwater localization problem [16], [17]. In [18], a floating model for double-head node was constructed to design a drifting restricted localization algorithm. Nevertheless, these mobility-based localization algorithms also face the clock synchronization assumption. How to design a mobility-based asynchronous localization algorithm to acquire the accurate localization of underwater sensor nodes is largely unexplored.

In this paper, we investigate the mobility-based asyn-

J. Yan, X. Zhang and X. Luo are with the Institute of Electrical Engineering, Yanshan University, Qinhuangdao 066004, China(e-mail: jyan@ysu.edu.cn, xnzhang@stumail.ysu.edu.cn, xyluo@ysu.edu.cn)

Y. Wang, C. Chen and X. Guan are with the Department of Automation, Shanghai Jiao Tong University, Shanghai 200240, China(email: yiyinwang@sjtu.edu.cn, xpguan@sjtu.edu.cn)

chronous localization problem for UASNs. We first provide a hybrid architecture for UASNs, which is composed of three types of nodes, i.e., autonomous underwater vehicles (AUVs), active sensor nodes, and passive sensor nodes. AUVs communicate with sensor nodes and provide the auxiliary information of localization. Active sensor nodes initiate the whole localization process by broadcasting localization messages to AUVs and passive sensor nodes. The passive sensor nodes listen to the messages and localize themselves without broadcasting any messages. An asynchronous localization algorithm with mobility prediction is then provided to estimate the locations of sensor nodes, where iterative least square estimators are carried out to solve the optimization problem. The main contributions of this paper are threefold.

- Unlike other algorithms assume the clock synchronization, we propose an asynchronous localization algorithm for UASNs. Meanwhile, the propagation delays on the way and from nodes are not necessarily equal.
- Considering the passive mobility of nodes, we provide a mobility prediction strategy to estimate the future location of sensor nodes. The localization accuracy in this paper can be improved comparing with the previous works.
- Iterative least square estimators are designed to solve the optimization problem, where Cramer-Rao lower bound and error analysis are also given. Compared with the exhaustive search-based localization method in [12], the localization time in this paper can be reduced.

The remainder of this paper is organized as follows: Section II includes the network architecture and an overview of the localization approach. The design of asynchronous localization approach is presented in Section III. In Section IV, position solution and performance analysis are given. Performance evaluations are provided in Section V, followed by a summary of conclusion and future works in Section VI.

II. Network Architecture and Overview of the Localization Approach

A. Network Architecture

The objective of the localization approach is to localize underwater sensor nodes through interactive communication and data processing. Due to the asynchronous clock and passive mobility of sensor nodes, how to obtain an accurate localization becomes a challenging issue. The UASNs in [19] realize localization by anchor nodes that float at the water surface. In special, underwater sensor nodes send information to anchor nodes frequently for localization calculation. However, considering the energy constraint and passive mobility of sensor nodes, the architecture in [19] can introduce localization errors while reducing the energy effectiveness for sensor nodes, especially for the nodes located at the bottom of UASNs. In [12], anchor nodes are deployed under the water surface to achieve the localization. Nevertheless, this architecture suffers from the error accumulation problem. Based on this, we propose a new network architecture that comprises of three different types of nodes, as shown in Fig. 1.

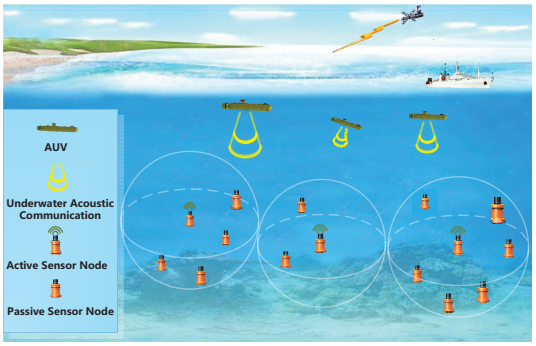

Fig. 1. The architecture of underwater acoustic sensor networks

- AUVs: AUVs are equipped with control theoretic navigation systems to obtain their locations through submerging and surfacing. When submerging into the water, AUVs act as anchor nodes to provide localization information for sensor nodes. Different from [9], AUVs are not assumed to be clock synchronized. With the submerging of AUVs, long-distance transmissions are replaced by short-distance ones, which means there exists less influence of noise and energy attenuation, such that sensors can obtain more accurate localization performance.
- Active sensor nodes: Active sensor nodes are capable of sensing, transmission and computation. They initiate the whole localization process by broadcasting localization messages to AUVs and passive sensor nodes. Due to the effect of current, active sensor nodes can move passively, whose task is to localize themselves with the proposed localization method in this paper.
- Passive sensor nodes: Passive sensor nodes are capable of sensing and computation. Without broadcasting any messages, they listen to the messages from AUVs and active sensor nodes. Similar to active sensor nodes, passive sensor nodes can move passively. The task of passive sensor nodes is to localize themselves with the proposed localization method in this paper.

B. Overview of the Localization Approach

The localization process is dividied into two subprocesses: active sensor node localization and passive sensor node localization. It is assumed that each sensor node is outfitted with a depth sensor, so with the range-based localization schemes, only the positions on X axis and Y axis need to be calculated to localize the active (or passive) sensor nodes. Inspired by this, three AUVs are assumed to be deployed to provide auxiliary localization information for sensor nodes.

At the beginning, AUVs float at the water surface and acquire their accurate locations through GPS. When the localization procedure begins, AUVs submerge and broadcast 'HELLO' message to the whole sensor network. After the 'HELLO' message is received by an active sensor node, the localization process for a sensor node can be given as follows.

1) At time $t_{s,s}$, active sensor node sends out an initialization message, which contains the sending order for AUVs, i.e., $n = 1, 2, 3$. Then, active sensor node switches into the waiting mode for the reply from AUVs.

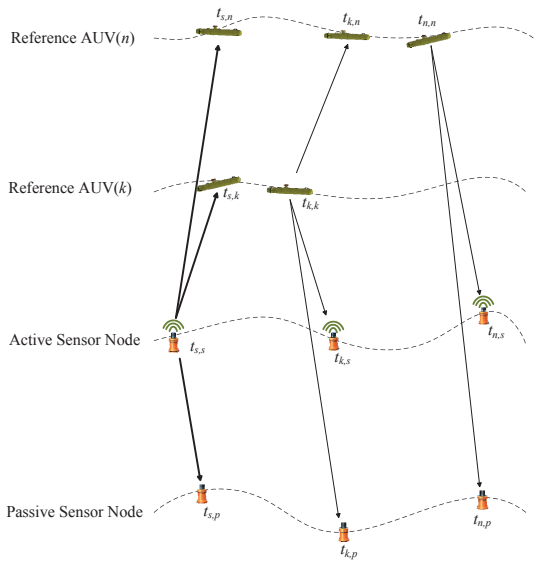

Fig. 2. The localization strategy

2) At time $t_{s,n}$, AUV n receives the initialization message. Then, AUV n switches into the listening mode and receives messages from AUV 1 to $n-1$, where the arrival times are denoted by $t_{k,n}$ $(k=1,...,n-1)$. Subsequently, at time $t_{n,n}$, AUV n sends out its localization message. In special, the localization message includes AUV ID n, $\{t_{k,n}\}_{\forall k}$, $t_{n,n}$, the position and velocity of AUV (which will be estimated in Section III-B).
3) At time $t_{n,s}$, active sensor node receives the reply from AUV n, where $n=1,...,3$. Similarly, the other AUV's replies can also be acquired, as shown in Fig. 2. After a complete round of localization transmission, the active sensor node has the following measurements

$$\{t_{s,n}, t_{n,n}, t_{n,s}\}_{n=1}^{3}, \quad \{t_{k,n}\}_{n=2,k=1}^{3,n-1}. \tag{1}$$

4) By receiving the localization message from active sensor node and the responding messages from AUVs, the passive sensor node has the following measurements

$$t_{s,p}, \{t_{s,n}, t_{n,p}, t_{n,n}\}_{n=1}^{3}, \{t_{k,n}, t_{k,p}\}_{n=2,k=1}^{3,n-1}. \tag{2}$$

5) With the collected localization messages, a mobility-based asynchronous localization algorithm is proposed to localize active and passive sensor nodes, wherein message broadcasting is not required for passive sensor node, as provided in Section III-C.

Given the previous discussions, the mobility-based asynchronous localization problem can now be stated as follows.

Problem: Considering the asynchronous clock and passive mobility constraints in underwater environment, we first provide a mobility prediction strategy to estimate the future locations of active and passive sensor nodes. Based on the predicted locations, an asynchronous localization algorithm is proposed to improve the localization accuracy, where iterative least square estimators are designed to solve the optimization problem such that the localization time can be reduced.

III. Asynchronous Localization Approach Design

In this section, we first construct the relationship between propagation delay and position. Then, a mobility prediction strategy is proposed for AUVs and sensor nodes to estimate their future positions. In the end, an asynchronous localization method is designed to acquire the position infomation.

A. Relationship between Propagation Delay and Position

Through message transmission process, active and passive sensor nodes acquire their timestamp measurements, as shown in (1) and (2). However, there exists a gap between the timestamp measurements and the understanding of localization. To bridge this gap, the relationship between propagation delay and position is required to be constructed.

For AUV n, the initial position is accurately acquired through GPS, where $n=1,2,3$. After the localization procedure begins, AUV n submerges and its real-time position is denoted by $(\mathcal{X}_n, \mathcal{Y}_n, \mathcal{Z}_n)$.[1] For an active sensor node, the initial and real-time positions are denoted by (x_s, y_s, z_s) and (x'_s, y'_s, z'_s), respectively. On the other hand, the initial and real-time positions of a passive sensor node are denoted by (x_p, y_p, z_p) and (x'_p, y'_p, z'_p), respectively.

With these denotations, the inital relative distance between active sensor node and AUV n is given as $d_{s,n}$, the inital relative distance between AUVs k and AUV n is $d_{k,n}$, while the inital relative distance between active and passive sensor nodes is $d_{s,p}$. Meanwhile, the real-time relative distance between AUV n and active sensor node is $d'_{n,s}$, and the real-time relative distance between AUV n and passive sensor node is $d'_{n,p}$. These relative distances are defined as follows:

$$\begin{cases} d_{s,n}=\sqrt{(x_s-\mathcal{X}_n)^2+(y_s-\mathcal{Y}_n)^2+(z_s-\mathcal{Z}_n)^2} \\ d_{k,n}=\sqrt{(\mathcal{X}_k-\mathcal{X}_n)^2+(\mathcal{Y}_k-\mathcal{Y}_n)^2+(\mathcal{Z}_k-\mathcal{Z}_n)^2} \\ d'_{n,s}=\sqrt{(\mathcal{X}_n-x'_s)^2+(\mathcal{Y}_n-y'_s)^2+(\mathcal{Z}_n-z'_s)^2} \\ d_{s,p}=\sqrt{(x_s-x_p)^2+(y_s-y_p)^2+(z_s-z_p)^2} \\ d'_{n,p}=\sqrt{(\mathcal{X}_n-x'_p)^2+(\mathcal{Y}_n-y'_p)^2+(\mathcal{Z}_n-z'_p)^2} \end{cases} \tag{3}$$

where the positions of sensor nodes on the Z axis (i.e., z_s, z_p, z'_s and z'_p) are assumed to be known through depth sensor. The positions of sensor nodes on the X axis and Y axis are unknown, which need to be computed.

Based on (3), the relationship between propagation delay and position is constructed as

$$\tau_{s,n} = \frac{d_{s,n}}{c}, \tau_{k,n} = \frac{d_{k,n}}{c}, \tag{4}$$

$$\tau'_{n,s} = \frac{d'_{n,s}}{c}, \tau_{s,p} = \frac{d_{s,p}}{c}, \tau'_{n,p} = \frac{d'_{n,p}}{c}, \tag{5}$$

where $c=1500$m/s is propagation speed of sound in water.

[1] In order to keep equations as clear as possible, the argument of time-dependent signals is omitted (e.g. $(\mathcal{X}_n, \mathcal{Y}_n, \mathcal{Z}_n) \equiv (\mathcal{X}_n(t), \mathcal{Y}_n(t), \mathcal{Z}_n(t))$). In addition, $(\mathcal{X}_n, \mathcal{Y}_n, \mathcal{Z}_n)$ is estimated with the mobility prediction strategy as provided in Section III-B.

B. Mobility Prediction for AUVs and Sensor Nodes

During the whole localization process, AUVs act as anchor nodes to provide auxiliary localization information for sensor nodes, and the position $(\mathcal{X}_n, \mathcal{Y}_n, \mathcal{Z}_n)$ is required to be known. Inpired by this, a linear prediction algorithm is first given to predict the positions of AUVs. Notice that $\mathcal{Z}_n$ can be acquired by pressure sensor installed on AUV, we only predict the vertical and horizontal positons, i.e., $\mathcal{X}_n$ and $\mathcal{Y}_n$.

For AUV n, the vertical and horizontal velocities at time instant t are denoted as $\mu_{n,x}(t)$ and $\mu_{n,y}(t)$, respectively. With a linear prediction algorithm, the predicted velocity is

$$\mu_n(t) = \sum_{m=1}^{l} a_m \mu_n(t - m\delta), \tag{6}$$

where $\mu_n(t-m\delta) = (\mu_{n,x}(t-m\delta), \mu_{n,y}(t-m\delta))$ is the velocity at time instant $t-m\delta$, l is the length of prediction step, and δ is the sampling period. a_m is the prediction coefficient, which can be obtained by the Dubin algorithm in [20].

With (6), the predicted position at time instant t is

$$(\mathcal{X}_n, \mathcal{Y}_n) = (\mathcal{X}_{n,start}, \mathcal{Y}_{n,start}) + \delta \sum_{j=0}^{l_{1,n}} \mu_n(t_{start} + j\delta), \tag{7}$$

where $(\mathcal{X}_{n,start}, \mathcal{Y}_{n,start})$ is the initial position of AUV n, and this position information can be accurately acquired through GPS because AUV n floats on water surface at the initial time instant. $l_{1,n} = (t - t_{start})/\delta$ is the total updating step till time instant t, and t_{start} is the initial time instant.

For sensor nodes, the initial positions are unknown, so the prediction algorithm of AUVs in (6) cannot be applied to sensor nodes. In [21], [22], it is pointed out that the movement of one object is closely related to its nearby objects according to the spatial correlations existed in underwater environments. Inspired by this, we use a common spatial correlation-based model [16], [23] to predict the mobility of sensor nodes. Let $v_{i,x}$ and $v_{i,y}$ denote the vertical and horizontal velocities of sensor node i, respectively. Thus, the predicted velocity of sensor node i is given as

$$\begin{array}{l} v_{i,x} = \sum_{j=1}^{3} \varsigma_{ij} \mu_{j,x} \\ v_{i,y} = \sum_{j=1}^{3} \varsigma_{ij} \mu_{j,y} \end{array}, \tag{8}$$

with

$$\varsigma_{ij} = \frac{\frac{1}{d_{ij}}}{\sum_{j=1}^{3} \frac{1}{d_{ij}}}, \tag{9}$$

where ς_{ij} is the interpolation coefficient, and d_{ij} is the distance between the sensor node i and AUV j.

In (9), the distance d_{ij} is required to be known. However, due to the impact of asynchronous clocks, sensor node i cannot directly obtain d_{ij} with the timestamp information in (1) and (2). To solve this issue, we attempt to establish the relationship between d_{ij} and localization information, such that d_{ij} can be indirectly acquired. In the following, we take the active sensor node as the example, where d_{ij} is refreshed as d'_{ns} (see Fig. 3). With the timestamp information in (1), we have

$$[(t_{n,s} - t_{s,s}) - (t_{n,n} - t_{s,n})]\, c = d_{sn} + d'_{ns} + w_{ns}, \tag{10}$$

where $t_{s,s}$ is the time instant when active sensor node begins to broadcast localization message, $t_{s,n}$ is the time instant when AUV n receives localization message, $t_{n,n}$ is the time instant

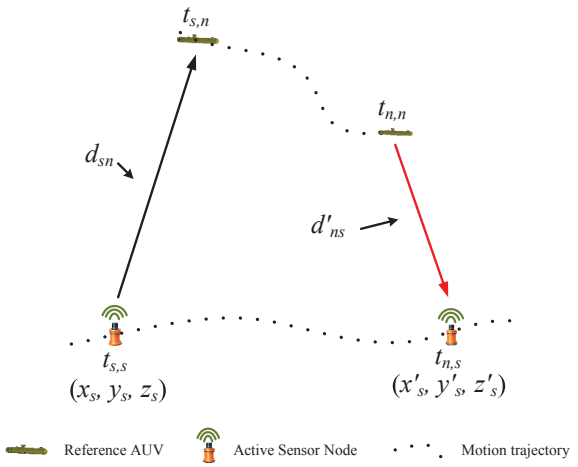

Fig. 3. The mobility of active sensor node.

when AUV n replies localization message, $t_{n,s}$ is the time instant when active sensor node receives the reply information from AUV n, d_{sn} is the relative distance of active sensor node and AUV n during the time interval $[t_{s,s},\ t_{s,n}]$, d'_{ns} is the relative distance of active sensor node and AUV n during the time interval $[t_{n,n},\ t_{n,s}]$, and w_{ns} is the equivalent noise.

According to the definitions in (3) and (4), it is obtained that d'_{ns} is related to the unknown initial position (x_s, y_s, z_s). Based on this, d'_{ns} can be expressed as a function of (x_s, y_s, z_s), and then v_s can also be expressed as a function of (x_s, y_s, z_s). In order to acquire the unknown variable (x_s, y_s, z_s), we define the asynchronous localization method (see Section III-C), whose solution is given in Section IV. With the solved variable (x_s, y_s, z_s), v_s can be obtained. Then, the relationship of (x'_s, y'_s) and (x_s, y_s) is constructed as

$$(x'_s, y'_s) = (x_s, y_s) + v_s(t_{n,s} - t_{s,s}). \tag{11}$$

Similarly, the relationship of (x'_p, y'_p) and (x_p, y_p) is constructed as

$$(x'_p, y'_p) = (x_p, y_p) + v_p(t_{n,p} - t_{s,p}), \tag{12}$$

where $t_{s,p}$ is the time instant when passive sensor node receives localization message from active sensor node, (x_p, y_p) is initial position of passive sensor node at time instant $t_{s,p}$, and $t_{n,p}$ is the time instant when passive node receives the reply information from AUV n.

C. Asynchronous Localization Method

Based on the timestamp information in (1) and (2), this section designs an asynchronous localization method for active and passive sensor nodes. The timestamp information can be described by Fig. 2. Without loss of generality, we ignore the clock skew and consider only with the clock offsets, where the similar assumption can also be found in [12].

In order to remove the effect of clock offsets, we define the following time differences for active sensor node, i.e.,

$$\Delta T_{n,s} = (t_{n,s} - t_{s,s}) - (t_{n,n} - t_{s,n}) \tag{13}$$

$$\Delta T_{k,n} = (t_{k,n} - t_{s,n}) - (t_{k,k} - t_{s,k}) \tag{14}$$

where $n = 1, 2, 3$ and $k = 1, ..., n-1$.

With (13) and (14), the relationship of time differences and propagation delays is established, i.e.,

$$\begin{aligned} \Delta T_{n,s} &= \tau_{s,n} + \tau'_{n,s} + w_{n,s} \\ \Delta T_{k,n} &= \tau_{s,k} + \tau_{k,n} - \tau_{s,n} + w_{k,n} \end{aligned} \tag{15}$$

where $w_{n,s}$ and $w_{k,n}$ are the measurement noises, and each time measurement is assumed to have variance δ^2_{mea}. Therefore, $w_{n,s}$ and $w_{k,n}$ satisfy the following distributions: $w_{n,s} \sim \mathcal{N}(0, 2\delta^2_{mea})$ and $w_{k,n} \sim \mathcal{N}(0, 3\delta^2_{mea})$.

Accordingly, the localization of active sensor node can be formulated as

$$\begin{aligned} &(\hat{x}_s, \hat{y}_s) \\ &= \text{argmin}_{(x_s,y_s)} \left\{ \tfrac{1}{4\delta^2_{mea}} \sum_{i=1}^{3} (\Delta T_{n,s} - \tau_{s,n} - \tau'_{n,s})^2 \right. \\ &\left. + \tfrac{1}{6\delta^2_{mea}} \sum_{n=2}^{3} \sum_{k=1}^{n-1} (\Delta T_{k,n} - \tau_{s,k} - \tau_{k,n} + \tau_{s,n})^2 \right\}. \end{aligned} \tag{16}$$

For passive sensor node, we define the following time differences

$$\begin{aligned} \Delta T_{s,n,p} &= (t_{n,p} - t_{s,p}) - (t_{n,n} - t_{s,n}), \\ \Delta T_{k,n,p} &= (t_{n,p} - t_{k,p}) - (t_{n,n} - t_{k,n}), \end{aligned} \tag{17}$$

where $n = 1, ..., 3$ and $k = 1, ..., n-1$.

Similar to (15), the relationship of time differences and propagation delays is established, i.e.,

$$\begin{aligned} \Delta T_{s,n,p} &= \tau_{s,n} + \tau'_{n,p} - \tau_{s,p} + w_{s,n,p}, \\ \Delta T_{k,n,p} &= \tau_{k,n} + \tau'_{n,p} - \tau'_{k,p} + w_{k,n,p}, \end{aligned} \tag{18}$$

where $w_{s,n,p}$ and $w_{k,n,p}$ are the measurement noises, which satisfy the following distributions: $w_{s,n,p} \sim \mathcal{N}(0, 3\delta^2_{mea})$ and $w_{k,n,p} \sim \mathcal{N}(0, 3\delta^2_{mea})$.

Then, the localization of passive sensor node can be formulated as

$$\begin{aligned} &(\hat{x}_p, \hat{y}_p) \\ &= \text{argmin}_{(x_p,y_p)} \tfrac{1}{6\delta^2_{mea}} \left\{ \sum_{n=2}^{3} \sum_{k=1}^{n-1} (\Delta T_{k,n,p} - \tau_{k,n} \right. \\ &\left. - \tau'_{n,p} + \tau'_{k,p})^2 + \sum_{n=1}^{3} (\Delta T_{s,n,p} - \tau_{s,n} - \tau'_{n,p} + \tau_{s,p})^2 \right\} \end{aligned} \tag{19}$$

IV. Position Solving and Performance Analysis

In this section, iterative least square estimators are designed to solve the optimization problems (16) and (19). In the end, performance analysis of the proposed approach is provided.

A. Position Solving for the Optimization Problem

For active sensor node, iterative least square method is applied to solve the optimization problem (16). As mentioned above, the time measurement is assumed to have variance δ^2_{mea}. Correspondingly, the variance on distance measurement is defined as $\delta^2_d = c^2\delta^2_{mea}$, where the propagation speed c is perfectly known. Hence, Eq. (16) is rearranged as

$$\begin{aligned} &(\hat{x}_s, \hat{y}_s) \\ &= \text{argmin}_{(x_s,y_s)} \left\{ \tfrac{1}{4\delta^2_d} \sum_{n=1}^{3} (c\Delta T_{n,s} - c\tau_{s,n} - c\tau'_{n,s})^2 \right. \\ &\left. + \tfrac{1}{6\delta^2_d} \sum_{n=2}^{3} \sum_{k=1}^{n-1} [c\Delta T_{k,n} - (c\tau_{s,k} + c\tau_{k,n} - c\tau_{s,n})]^2 \right\}. \end{aligned} \tag{20}$$

Considering the conditions in (4) and (5), we rearrange (15) and have the following results, i.e.,

$$\underbrace{\begin{bmatrix} \frac{c\Delta T_{1,s}}{2} \\ \frac{c\Delta T_{2,s}}{2} \\ \frac{c\Delta T_{3,s}}{2} \\ \frac{c\Delta T_{1,2}}{\sqrt{6}} \\ \frac{c\Delta T_{1,3}}{\sqrt{6}} \\ \frac{c\Delta T_{2,3}}{\sqrt{6}} \end{bmatrix}}_{:=\varphi_1} = \underbrace{\begin{bmatrix} \frac{d_{s,1}+d'_{1,s}}{2} \\ \frac{d_{s,2}+d'_{2,s}}{2} \\ \frac{d_{s,3}+d'_{3,s}}{2} \\ \frac{d_{s,1}+d_{1,2}-d_{s,2}}{\sqrt{6}} \\ \frac{d_{s,1}+d_{1,3}-d_{s,3}}{\sqrt{6}} \\ \frac{d_{s,2}+d_{2,3}-d_{s,3}}{\sqrt{6}} \end{bmatrix}}_{:=h_1} + \underbrace{\begin{bmatrix} \frac{cw_{1,s}}{2} \\ \frac{cw_{2,s}}{2} \\ \frac{cw_{3,s}}{2} \\ \frac{cw_{1,2}}{\sqrt{6}} \\ \frac{cw_{1,3}}{\sqrt{6}} \\ \frac{cw_{2,3}}{\sqrt{6}} \end{bmatrix}}_{:=W_1} \tag{21}$$

From (21), the following nonlinear relation is constructed:

$$\varphi_1 = h_1(\eta_1, \xi) + W_1. \tag{22}$$

where $h = h_1(\eta_1, \xi_n) \in \mathcal{R}^{6\times 1}$, $\eta_1 = (x_s, y_s)$ denotes position of active sensor node, $\xi = [\mathcal{X}_1, \mathcal{Y}_1; \mathcal{X}_2, \mathcal{Y}_2; \mathcal{X}_3, \mathcal{Y}_3]$ is the real-time position matrix of AUVs.

To solve the nonlinear estimation in (22), we carry out the Taylor series expansion. Then, we have

$$\varphi_1 = h_1(\hat{\eta}^i_1, \xi) + J_1\delta_1 + W_1 \tag{23}$$

where $\hat{\eta}^i_1$ is the estimation in the ith iteration. J_1 is the Jacobian matrix, i.e.,

$$J_1 = \frac{\partial h_1(\eta_1, \xi)}{\partial \eta_1} \mid_{\eta_1 = \hat{\eta}^i_1},$$

which can be expressed as

$$J_1 = \begin{bmatrix} \frac{1}{2}(\frac{x_s-\mathcal{X}_1}{d_{s,1}} + \frac{x'_s-\mathcal{X}_1}{d'_{1,s}}) & \frac{1}{2}(\frac{y_s-\mathcal{Y}_1}{d_{s,1}} + \frac{y'_s-\mathcal{Y}_1}{d'_{1,s}}) \\ \frac{1}{2}(\frac{x_s-\mathcal{X}_2}{d_{s,2}} + \frac{x'_s-\mathcal{X}_2}{d'_{2,s}}) & \frac{1}{2}(\frac{y_s-\mathcal{Y}_2}{d_{s,2}} + \frac{y'_s-\mathcal{Y}_2}{d'_{2,s}}) \\ \frac{1}{2}(\frac{x_s-\mathcal{X}_3}{d_{s,3}} + \frac{x'_s-\mathcal{X}_3}{d'_{3,s}}) & \frac{1}{2}(\frac{y_s-\mathcal{Y}_3}{d_{s,3}} + \frac{y'_s-\mathcal{Y}_3}{d'_{3,s}}) \\ \frac{1}{\sqrt{6}}(\frac{x_s-\mathcal{X}_1}{d_{s,1}} - \frac{x_s-\mathcal{X}_2}{d_{s,2}}) & \frac{1}{\sqrt{6}}(\frac{y_s-\mathcal{Y}_1}{d_{s,1}} - \frac{y_s-\mathcal{Y}_2}{d_{s,2}}) \\ \frac{1}{\sqrt{6}}(\frac{x_s-\mathcal{X}_1}{d_{s,1}} - \frac{x_s-\mathcal{X}_3}{d_{s,3}}) & \frac{1}{\sqrt{6}}(\frac{y_s-\mathcal{Y}_1}{d_{s,1}} - \frac{y_s-\mathcal{Y}_3}{d_{s,3}}) \\ \frac{1}{\sqrt{6}}(\frac{x_s-\mathcal{X}_2}{d_{s,2}} - \frac{x_s-\mathcal{X}_3}{d_{s,3}}) & \frac{1}{\sqrt{6}}(\frac{y_s-\mathcal{Y}_2}{d_{s,2}} - \frac{y_s-\mathcal{Y}_3}{d_{s,3}}) \end{bmatrix}.$$

So the iterative least squares increment δ_1 is

$$\delta_1 = \left[J_1^T R_1^{-1} J_1\right]^{-1} J_1^T R_1^{-1} D_1, \tag{24}$$

where $\delta_1 = [\delta_{1x}, \delta_{1y}]^T$, $D_1 = [\varphi_1[1] - h_1(\hat{\eta}^i_1, \xi),\ \varphi_1[2] - h_1(\hat{\eta}^i_1, \xi), \ldots, \varphi_1[6] - h_1(\hat{\eta}^i_1, \xi)]^T$, R_1 is the covariance matrix of the term W_1.

Based on the estimate $\hat{\eta}^i_1$ in the ith iteration, the estimate in the $(i+1)$st iteration is updated as

$$\hat{\eta}^{i+1}_1 = \hat{\eta}^i_1 + \delta_1, \tag{25}$$

After a sufficient number of iterations, the position vector $\eta_1 = [x_s, y_s]^T$ for active sensor node can be obtained, and the mean square error (MSE) matrix can be obtained as

$$E\left[(\hat{\eta}^i_1 - \eta_1)^T(\hat{\eta}^i_1 - \eta_1)\right] = (J_1^T R_1^{-1} J_1)^{-1}. \tag{26}$$

In the following, we use iterative least square method to solve the optimization problem (19). Similarly, (19) can be rearranged as

$$\begin{aligned} &(\hat{x}_p, \hat{y}_p) \\ &= \text{argmin}_{(x_p,y_p)} \left\{ \tfrac{1}{6\delta^2_d} \sum_{n=2}^{3} \sum_{k=1}^{n-1} [c\Delta T_{k,n,p} - (d_{k,n} + d'_{n,p} \right. \\ &\left. - d'_{k,p})]^2 + \tfrac{1}{6\delta^2_d} \sum_{n=1}^{3} [c\Delta T_{s,n,p} - (d_{s,n} + d'_{n,p} - d_{s,p})]^2 \right\} \end{aligned} \tag{27}$$

According to the relationship in (5) and (18), we have

$$\underbrace{\begin{bmatrix} c\Delta T_{1,2,p} \\ c\Delta T_{1,3,p} \\ c\Delta T_{2,3,p} \\ c\Delta T_{s,1,p} \\ c\Delta T_{s,2,p} \\ c\Delta T_{s,3,p} \end{bmatrix}}_{:=\varphi_2} = \underbrace{\begin{bmatrix} (d_{1,2}+d'_{2,p}-d'_{1,p}) \\ (d_{1,3}+d'_{3,p}-d'_{1,p}) \\ (d_{2,3}+d'_{3,p}-d'_{2,p}) \\ (d_{s,1}+d'_{1,p}-d_{s,p}) \\ (d_{s,2}+d'_{2,p}-d_{s,p}) \\ (d_{s,3}+d'_{3,p}-d_{s,p}) \end{bmatrix}}_{:=h_2} + \underbrace{\begin{bmatrix} cw_{1,2,p} \\ cw_{1,3,p} \\ cw_{2,3,p} \\ cw_{s,1,p} \\ cw_{s,2,p} \\ cw_{s,3,p} \end{bmatrix}}_{:=W_2} \tag{28}$$

From (28), the following nonlinear relation is constructed

$$\varphi_2 = h_2 + W_2, \tag{29}$$

where $h_2 = h_2(\eta_2, \xi)$, and $\eta_2 = (x_p, y_p)$ denotes the position of passive sensor node.

Similar to (23), one has

$$\varphi_2 = h_2(\hat{\eta}_2^i, \xi_2) + J_2\delta_2 + W_2 \tag{30}$$

where $\hat{\eta}_2^i$ is the estimate in the ith iteration, and J_2 is the Jacobian matrix, i.e.,

$$J_2 = \frac{\partial h_2(\eta_2, \xi_2)}{\partial \eta_2} \mid_{\eta_2=\hat{\eta}_2^i}, \tag{31}$$

which is expressed as

$$J_2 = \begin{bmatrix} \frac{\mathcal{X}_1-x'_p}{d'_{1,p}} - \frac{\mathcal{X}_2-x'_p}{d'_{2,p}} & \frac{\mathcal{Y}_1-y'_p}{d'_{1,p}} - \frac{\mathcal{Y}_2-y'_p}{d'_{2,p}} \\ \frac{\mathcal{X}_1-x'_p}{d'_{1,p}} - \frac{\mathcal{X}_3-x'_p}{d'_{3,p}} & \frac{\mathcal{Y}_1-y'_p}{d'_{1,p}} - \frac{\mathcal{Y}_3-y'_p}{d'_{3,p}} \\ \frac{\mathcal{X}_2-x'_p}{d'_{2,p}} - \frac{\mathcal{X}_3-x'_p}{d'_{3,p}} & \frac{\mathcal{Y}_2-y'_p}{d'_{2,p}} - \frac{\mathcal{Y}_3-y'_p}{d'_{3,p}} \\ \frac{x_s-x_p}{d_{s,p}} - \frac{\mathcal{X}_1-x'_p}{d'_{1,p}} & \frac{y_s-x_p}{d_{s,p}} - \frac{\mathcal{Y}_1-y'_p}{d'_{1,p}} \\ \frac{x_s-x_p}{d_{s,p}} - \frac{\mathcal{X}_2-x'_p}{d'_{2,p}} & \frac{y_s-y_p}{d_{s,p}} - \frac{\mathcal{Y}_2-y'_p}{d'_{2,p}} \\ \frac{x_s-x_p}{d_{s,p}} - \frac{\mathcal{X}_3-x'_p}{d'_{3,p}} & \frac{y_s-y_p}{d_{s,p}} - \frac{\mathcal{Y}_3-y'_p}{d'_{3,p}} \end{bmatrix}. \tag{32}$$

Thus, the iterative least squares increment is

$$\delta_2 = \left[J_2^T R_2^{-1} J_2\right]^{-1} J_2^T R_2^{-1} D_2, \tag{33}$$

where $\delta_2 = [\delta_{2x}, \delta_{2y}]^T$, $D_2 = [\varphi_2[1] - h(\hat{\eta}_2^i, \xi_2), \varphi_2[2] - h_2(\hat{\eta}_2^i, \xi_2), \ldots, \varphi_2[6] - h_2(\hat{\eta}_2^i, \xi_2)]$, and R_2 is the covariance matrix of the term W_2.

Based on the estimate $\hat{\eta}_2^i$ in the ith iteration, the estimate in the $(i+1)$st iteration is updated as

$$\hat{\eta}_2^{i+1} = \hat{\eta}_2^i + \delta_2. \tag{34}$$

After a sufficient number of iterations, the position vector $\eta_2 = [x_p, y_p]^T$ for passive sensor node can be obtained, and the MSE matrix is given as

$$E\left[(\hat{\eta}_2^i - \eta_2)^T(\hat{\eta}_2^i - \eta_2)\right] = (J_2^T R_2^{-1} J_2)^{-1}. \tag{35}$$

B. Performance Analysis

In this section, we first drive the Cramer-Rao lower bound (CRB) for the proposed localization algorithm. As discussed in [24], [25], CRB is a lower bound to the error variance of any parameter estimator, which serves as an important tool in the performance evaluation of estimators.

Given an unknown vector η, the log-likelihood function is denoted as $\ln \Lambda(\eta)$, and the the ground truth is η_0. Then, the Fisher Information Matrix (FIM) is given as

$$\begin{aligned} I(\eta) &= E\left\{[\bigtriangledown_\eta \ln \Lambda(\eta)]\,[\bigtriangledown_\eta \ln \Lambda(\eta)]^T\right\} \mid_{\eta=\eta_0} \\ &= -E\left\{\bigtriangledown_\eta \bigtriangledown_\eta^T \ln \Lambda(\eta)\right\} \mid_{\eta=\eta_0}, \end{aligned} \tag{36}$$

where $E\{\cdot\}$ is the expectation.

Correspondingly, the CRLB can be defined as

$$C_{RLB}(\eta) = I^{-1}(\eta). \tag{37}$$

For facilitation of the description, the real-time positions of active sensor node, passive sensor node and AUV n in vertical and horizontal axes are denoted as $\eta'_1 = [x'_s, y'_s]^T$, $\eta'_2 = [x'_p, y'_p]^T$ and $l_n = [\mathcal{X}_n, \mathcal{Y}_n]^T$, respectively. As the position in depth axis can be acquired by pressure sensor, we only analyze the estimation performance in vertical and horizontal axes.

1) The CRB for Active Sensor Node

For active sensor node, $l_n = [\mathcal{X}_n, \mathcal{Y}_n]^T$ is the collected measurement. In addition, η_1 and η'_1 satisfy the relationship in (11), wherein η_1 is required to be calculated. Referring to [24], the log likelihood function is constructed as

$$\begin{aligned} &\ln \Lambda_1(\eta_1) \\ =\ & \frac{1}{4\delta_d^2} \sum_{n=1}^{3} \left(c\Delta T_{n,s} - \|l_n - \eta_1\| - \|l_n - \eta'_1\|\right)^2 \\ & + \frac{1}{6\delta_d^2} \sum_{n=2}^{3} \sum_{k=1}^{n-1} [c\Delta T_{k,n} - (\|l_k - \eta_1\| \\ & + \|l_k - l_n\| - \|l_n - \eta_1\|)]^2. \end{aligned} \tag{38}$$

Based on (36), the FIM for $\ln \Lambda_1(\eta_1)$ is defined as $I_1(\eta_1) \in \mathcal{R}^{2\times 2}$. With straightforward derivation, we have

$$\begin{aligned} [I_1]_{1,1} &= \frac{1}{2\delta_d^2} \sum_{n=1}^{3} \left[\frac{(\mathcal{X}_n - x_s)}{\|l_n - \eta_1\|} - \frac{(\mathcal{X}_n - x'_s)}{\|l_n - \eta'_1\|}\right]^2 \\ &\quad + \frac{1}{3\delta_d^2} \sum_{n=2}^{3} \sum\nolimits_{k=1}^{n-1} \left[\frac{(\mathcal{X}_n - x_s)}{\|l_n - \eta_1\|} - \frac{(\mathcal{X}_k - x_s)}{\|l_k - \eta_1\|}\right]^2, \\ [I_1]_{2,2} &= \frac{1}{2\delta_d^2} \sum_{n=1}^{3} \left[\frac{(\mathcal{Y}_n - y_s)}{\|l_n - \eta_1\|} - \frac{(\mathcal{Y}_n - y'_s)}{\|l_n - \eta'_1\|}\right]^2 \\ &\quad + \frac{1}{3\delta_d^2} \sum_{n=2}^{3} \sum_{k=1}^{n-1} \left[\frac{(\mathcal{Y}_n - y_s)}{\|l_n - \eta_1\|} - \frac{(\mathcal{Y}_k - y_s)}{\|l_k - \eta_1\|}\right]^2, \\ [I_1]_{1,2} &= [I_1]_{2,1} = \frac{1}{2\delta_d^2} \sum_{n=1}^{3} \left[\frac{(\mathcal{X}_n - x_s)}{\|l_n - \eta_1\|} - \frac{(\mathcal{X}_n - x'_s)}{\|l_n - \eta'_1\|}\right] \\ &\quad \times \left[\frac{(\mathcal{Y}_n - y_s)}{\|l_n - \eta_1\|} - \frac{(\mathcal{Y}_n - y'_s)}{\|l_n - \eta'_1\|}\right] \\ &\quad + \frac{1}{3\delta_d^2} \sum\nolimits_{n=2}^{3} \sum\nolimits_{k=1}^{n-1} \left[\frac{(\mathcal{X}_n - x_s)}{\|l_n - \eta_1\|} - \frac{(\mathcal{X}_k - x_s)}{\|l_k - \eta_1\|}\right] \\ &\quad \times \left[\frac{(\mathcal{Y}_n - y_s)}{\|l_n - \eta_1\|} - \frac{(\mathcal{Y}_k - y_s)}{\|l_k - \eta_1\|}\right]. \end{aligned}$$

Hence, the solution from (20) has position error

$$E\left\{\|\hat{\eta}_1 - \eta_1\|^2\right\} \geq \mathrm{tr}\left\{I_1^{-1}(\eta)\right\}\big|_{\eta=\eta_1}, \tag{39}$$

where $\mathrm{tr}\{\cdot\}$ denotes the trace of a matrix.

2) The CRB for Passive Sensor Node

For passive sensor node, η_2 and η_2' satisfy the relationship in (12), wherein η_2 is required to be calculated. Similar to (38), the log likelihood function is constructed as

$$\begin{aligned}&\ln\Lambda_2(\eta_2)\\ =\ &\tfrac{1}{6\delta_d^2}\sum_{n=2}^{3}\sum_{k=1}^{n-1}c\Delta T_{k,n,p}-(\|l_k-l_n\|+\|l_n-\eta_2'\|\\ &-\|l_n-\eta_2'\|)^2+\tfrac{1}{6\delta_d^2}\sum_{n=1}^{3}[c\Delta T_{s,n,p}-(\|l_n-\eta_1\|\\ &+\|l_n-\eta_2'\|-\|\eta_1-\eta_2\|)]^2. \end{aligned}\tag{40}$$

Hence, the FIM for $\ln\Lambda_2(\eta_2)$ can be defined as $I_2(\eta_2)\in\mathcal{R}^{2\times2}$. With straightforward derivation, one obtains

$$\begin{aligned}[I_2]_{1,1} &= \frac{1}{3\delta_d^2}\sum_{n=2}^{3}\sum_{k=1}^{n-1}\left[\frac{(\mathcal{X}_n-x_p')}{\|l_n-\eta_2'\|}-\frac{(\mathcal{X}_k-x_p')}{\|l_k-\eta_2'\|}\right]^2\\ &\quad+\frac{1}{3\delta_d^2}\sum_{n=1}^{3}\left[\frac{(\mathcal{X}_n-x_p')}{\|l_n-\eta_2'\|}-\frac{(x_s-x_p)}{\|l_s-\eta_2\|}\right]^2,\\ [J_2]_{2,2} &= \frac{1}{3\delta_d^2}\sum_{n=2}^{3}\sum_{k=1}^{n-1}\left[\frac{(\mathcal{Y}_n-y_p')}{\|l_n-\eta_2'\|}-\frac{(\mathcal{Y}_k-y_p')}{\|l_k-\eta_2'\|}\right]^2\\ &\quad+\frac{1}{3\delta_d^2}\sum_{n=1}^{3}\left[\frac{(\mathcal{Y}_n-y_p')}{\|l_n-\eta_2'\|}-\frac{(y_s-y_p)}{\|l_s-\eta_2\|}\right]^2,\\ [J_2]_{1,2} &= [J_2]_{2,1}=\frac{1}{3\delta_d^2}\sum_{n=2}^{3}\sum_{k=1}^{n-1}\left[\frac{(\mathcal{X}_n-x_p')}{\|l_n-\eta_2'\|}\right.\\ &\quad\left.-\frac{(\mathcal{X}_k-x_p')}{\|l_k-\eta_2'\|}\right]\left[\frac{(\mathcal{Y}_n-y_p')}{\|l_n-\eta_2'\|}-\frac{(\mathcal{Y}_k-y_p')}{\|l_k-\eta_2'\|}\right]\\ &\quad+\frac{1}{3\delta_d^2}\sum_{n=1}^{3}\left[\frac{(\mathcal{X}_n-x_p')}{\|l_n-\eta_2'\|}-\frac{(x_s-x_p)}{\|l_s-\eta_2\|}\right]\\ &\quad\times\left[\frac{(\mathcal{Y}_n-y_p')}{\|l_n-\eta_2'\|}-\frac{(y_s-y_p)}{\|l_s-\eta_2\|}\right].\end{aligned}$$

Therefore, the solution from (27) has position error

$$E\left\{\|\hat{\eta}_2-\eta_2\|^2\right\}\geq \mathrm{tr}\left\{I_2^{-1}(\eta)\right\}\big|_{\eta=\eta_2}.\tag{41}$$

V. Simulation Results

In this section, simulation results are given to demonstrate the performance of the asynchronous localization approach.

A. Simulation Settings

The simulations are implemented in MATLAB 2016b. Several assumptions with regard to the capabilities of the modems and the communications channel are made. It is assumed that AUVs can efficiently communicate with active and passive sensor nodes, while the data packets during the the communication process can be successfully received and decoded. Without loss of generality, we only consider the timing estimation noises at the receiver nodes. In the simulation, three AUVs, one active sensor node and eight passive sensor nodes are deployed in an area of 1000m×1000m×1000m.

At the beginning, AUVs float at the water surface and acquire their accurate locations through GPS. When the localization procedure begins, AUVs submerge and act as anchor nodes to provide localization information for sensor nodes. The following underwater kinematic model [26], [27] is adopted to provide initial velocities for AUVs, i.e.,

$$\begin{cases}\mu_x=k_l\lambda v\sin(k_2x)\cos(k_3y)+k_1\lambda\cos(2k_lt)+k_4\\ \mu_y=-\lambda v\sin(k_3x)\cos(k_2y)+k_5,\end{cases}$$

where μ_x and μ_y are the velocities in X axis and Y axis, respectively. k_1, k_2, k_3, λ and v are random variables which are related to the underwater environment factors such as tides and bathymetry. k_4 and k_5 are positive parameters. In special, it is assumed that k_1, k_2, k_3, λ and v are subject to the normal distributions, while k_4 and k_5 are constants. The detailed values of these parameters are shown in Table I.

TABLE I
Simulation Parameters Used in the Simulation.

Parameter	Value	Parameter	Value
k_1	$\mathcal{N}(0.001\pi,0.0001\pi)$	k_2	$\mathcal{N}(0.01\pi,0.001\pi)$
k_3	$\mathcal{N}(0.02\pi,0.002\pi)$	k_4	0.015
k_5	0.01	λ	$\mathcal{N}(1,0.1)$
v	$\mathcal{N}(0.1,0.01)$		

B. Results and Analysis

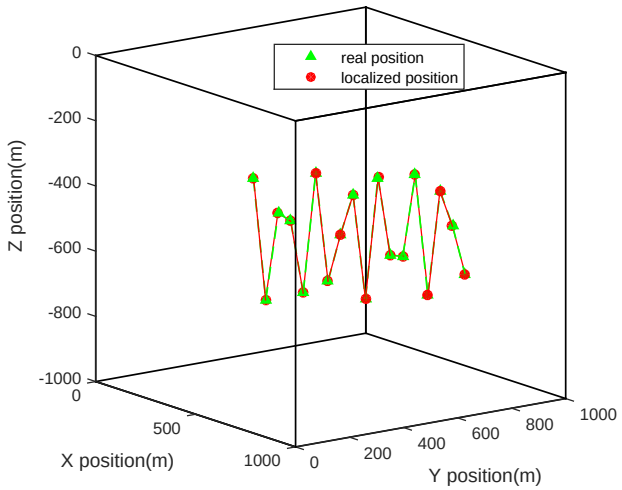

Fig. 4. The real and localized trajectories of an active sensor node.

1) Localization trajectory of an active sensor node

As mentioned above, sensor nodes can move passively due to the effect of current. In this paper, the movements of active and passive sensor nodes are closely related to their nearby AUVs according to the spatial correlations existed in underwater environments. Under this case, the real trajectory of an active sensor node is shown in Fig. 4. By using the asynchronous localization approach in Section III-C, the localized trajectory is also given in Fig. 4. To show more clearly, a localization error function $\mathrm{DEV}_s=\sqrt{(x_s-\hat{x}_s)^2+(y_s-\hat{y}_s)^2+(z_s-\hat{z}_s)^2}$ is defined, where $(\hat{x}_s,\hat{y}_s,\hat{z}_s)$ is the calculated location of the active sensor node and (x_s,y_s,z_s) is the real location of the active sensor node. Notice that z_s can be acquired by pressure sensor, and the main focus in this paper is the

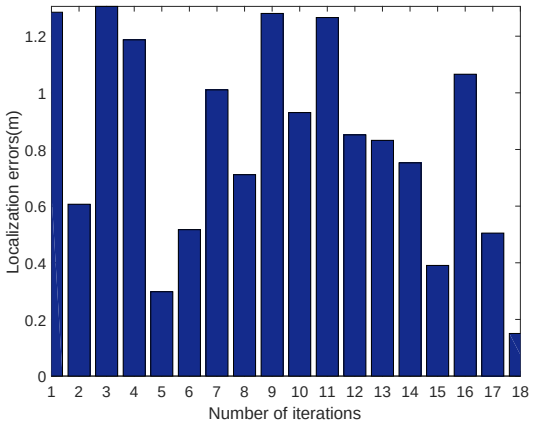

Fig. 5. The localization error for an active sensor node.

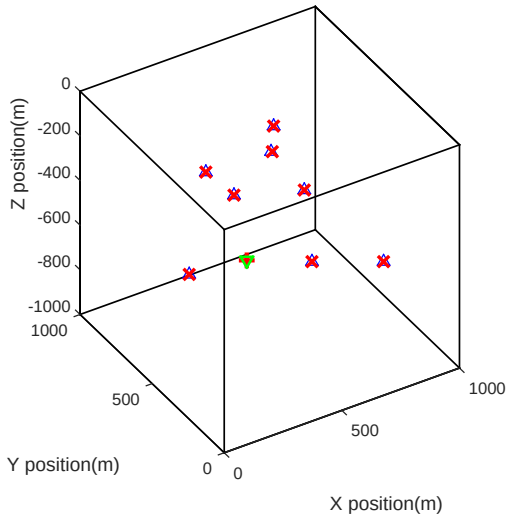

Fig. 6. Localization of the active and passive sensor nodes.

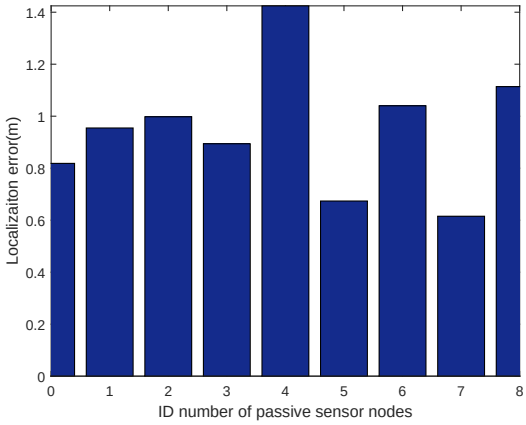

Fig. 7. The localization error for the active and passive sensor nodes, where the ID number 1 for active sensor node, and the other ones are for passive sensor nodes.

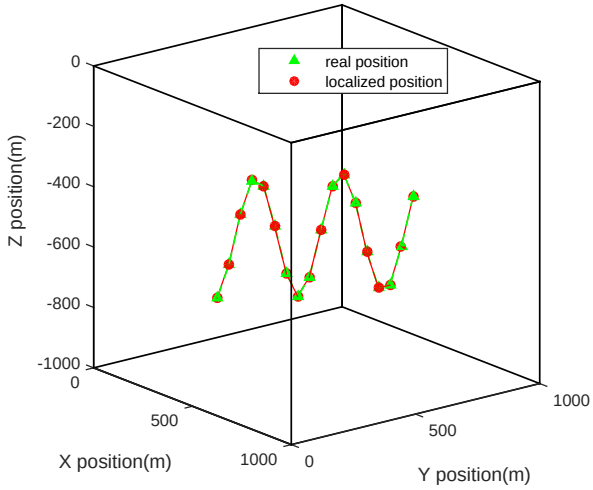

Fig. 8. The real and localized trajectories of a passive sensor node.

localization algorithm. Hence, it is assumed that pressure sensor can accurately measure the depth information, i.e., $z_s = \hat{z}_s$. Correspondingly, the localization errors are shown in Fig. 5. Clearly, the localization task for an active sensor node can be achieved.

2) Localization of the UASNs

In our simulation, one active sensor node and eight passive sensor nodes are deployed. We apply the asynchronous localization approach to all sensor nodes. Hence, the real and localized positions of these nodes are shown in Fig. 6. The localization errors are provided in Fig. 7, where the reversed triangle denotes the real position of active sensor node, the regular triangle is for the real position of passive sensor nodes, the plus sign shows the localized position of active sensor node, and the cross sign shows the localized position of passive sensor node. It is seen that the localization task for the whole nodes in UASNs can be achieved.

3) Localization trajectory of a passive sensor node

With the proposed localization method in this paper, the trajectory of an passive sensor node can also be estimated. Inspired by this, the real and localized trajectories of a passive sensor node is shown in Fig. 8. Meanwhile, the localization errors are shown in Fig. 9. Obvioulsy, the localization task for a passive sensor node can be achieved.

4) Error analysis of reference AUVs

In the localization process, AUVs act as anchor nodes to provide localization information for sensor nodes, and the reference messages provided by AUV affect the accuracy of the localization results. The reference messages include time stamps, AUV's position and velocity. The error of time stamps is associated with the measurement error and underwater communication noise. The errors of position and velocity influence the accuracy of mobility prediction in Section III-B. To verify this conclusion, noises are added to the velocity and position information povided by AUVs. Fig. 10 shows the localization errors of an active sensor nodes when the velocity information provided by AUV is not accurate. When the positon information provided by AUV is not accurate, the localization errors of an active sensor node are shown in

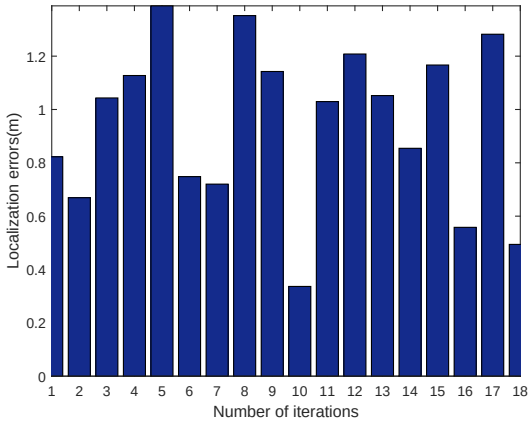

Fig. 9. The localization error for a passive sensor node.

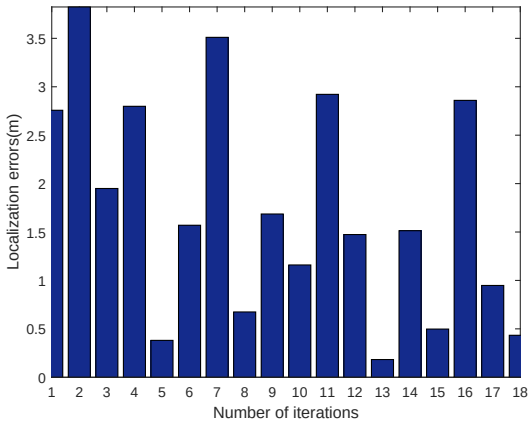

Fig. 10. Localization errors when the velocity information provided by AUVs is not accurate.

Fig. 11. Clearly, the accuracy of localization is not good. The similar can also be obtained by the passive sensor nodes. In order to reduce this negative impact, AUVs are required to surface and re-localize themselves with the assistant of GPS.

5) Comparison with mobility-based localization algorithm

In [16], a scalable localizaiton algorithm with mobility prediction (SLMP) was proposed for UASNs. However, the clock in [16] is assumed to be synchronized. Under synchronous assumption, we apply the SLMP-based localization approach to localize an active sensor node, and the localization errors are shown in Fig. 12. Under the same assumption and noises, we apply the localization approach in this paper to localize the active sensor node, and the localization errors are also given in Fig. 12. Clearly, the localization task can be achieved with the above two methods. However, the clock in underwater environment is always asynchronous. When the clock is asynchronous, the clock offset is set to be randomly initialized from 1ms to 200ms. Hence, the localized trajectories of the UASNs by using the SLMP-based localization approach is shown in Fig. 13. To show more clearly, the localization errors are given in Fig. 14. Clearly, the asynchronous clock seriously affects the localization accuracy and the localization task can be achieved.

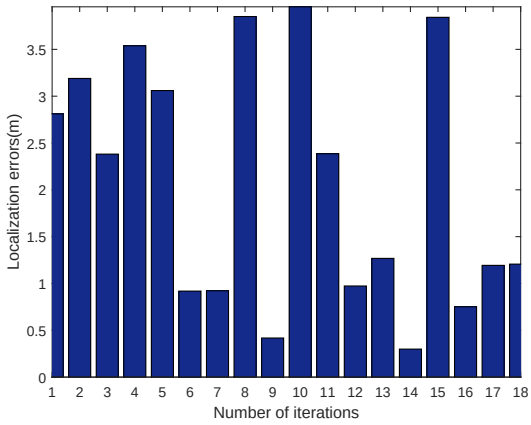

Fig. 11. Localization errors when the position information provided by AUVs is not accurate.

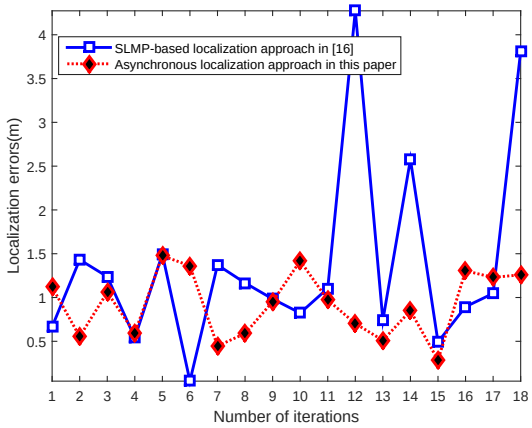

Fig. 12. Under synchronous assumption, localization errors with SLMP-based localization approach in [16] and the approach in this paper.

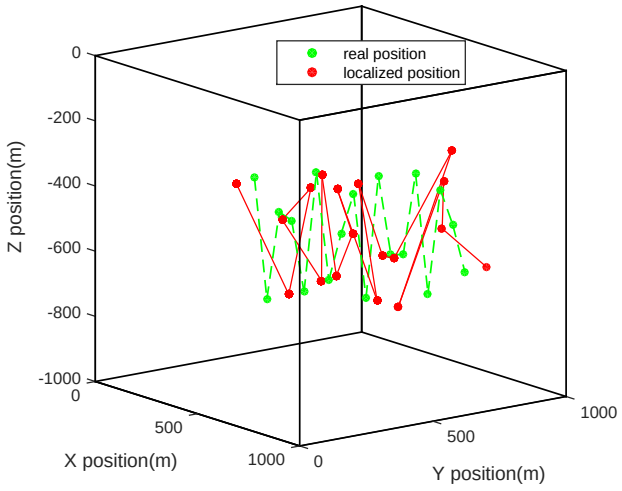

Fig. 13. Under asynchronous clock, localization trajectories with SLMP-based localization approach in [16].

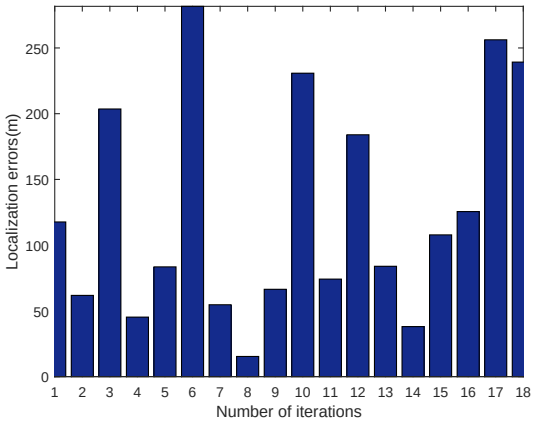

Fig. 14. Under asynchronous clock, localization errors with SLMP-based localization approach in [16].

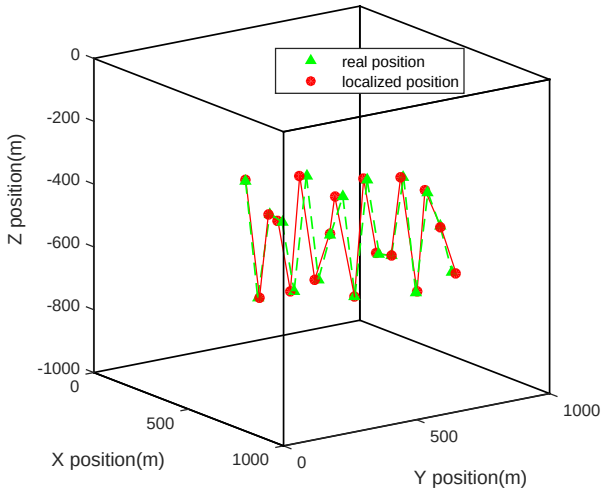

Fig. 17. Under mobile UASNs, localization trajectories with OADL-based localization approach in [12].

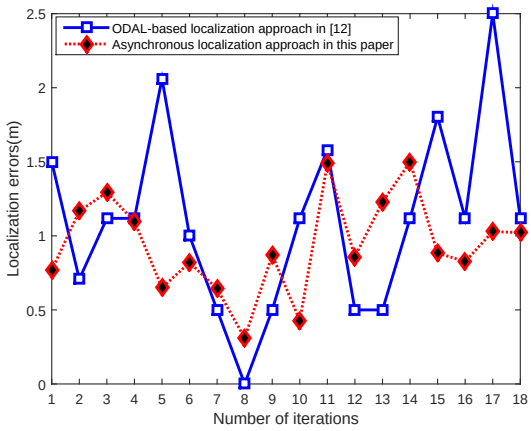

Fig. 15. Under static UASNs, localization errors with OADL-based localization approach in [12] and the approach in this paper.

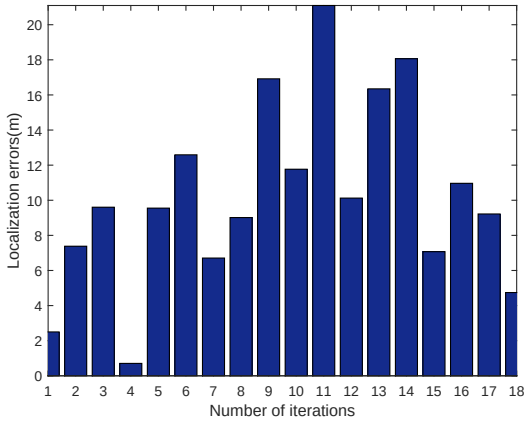

Fig. 18. Under mobile UASNs, localization errors with OADL-based localization approach in [12]

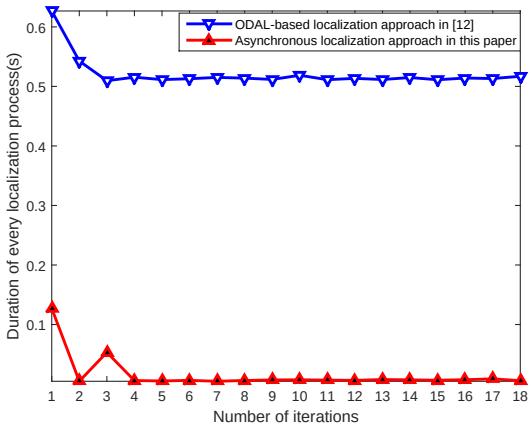

Fig. 16. Under static UASNs, durations with OADL-based localization approach in [12] and the approach in this paper.

Alternatively, the asynchronous algorithm in this paper can effectively eliminate the impact of the clock asynchronization, i.e., the localization task can be achieved by using the method in this paper (see Fig. 6 and Fig. 7).

6) Comparison with asynchronous localization algorithm

In [12], an on-demand asynchronous localization approach (ODAL) was proposed for UASNs, where exhaustive search is used to find the solution. However, the nodes in [16] are assumed to be static, while the duration of localization in exhaustive search is long because a large amount of computation is required. Under static assumption, we apply the ODAL-based localization approach to localize an active sensor node, and the localization errors are shown in Fig. 15. Under the same assumption and noises, we apply the localization approach in this paper to localize the active sensor node, and the localization errors are also given in Fig. 15. Clearly, the localization task can be achieved with the above two methods. The durations of the two approaches are shown in Fig. 16. Compared with the exhaustive search-based localization

method in [12], the localization time with iterative least square in this paper can be reduced. On the other hand, mobility in underwater environment must be considered, as the sensor nodes often have passive mobility caused by water current or tides. In such a situation, we apply the ODAL algorithm to a mobile UASN. Fig. 17 shows the localization trajectory of an active sensor node, and the localization errors are given in Fig. 18. Clearly, the localization accuracy of ODAL declines and the localization task cannot be achieved.

VI. Conclusion and Future Work

In this paper, we present an asynchronous localization algorithm with mobility prediction for UASNs. The algorithm includes the mobility of sensor nodes with the help of AUVs, an asynchronous algorithm for sensor nodes to localize themselves, and an iterative least squares method to solve the optimization problem. Based on simulations and analysis of the Cramer-Rao lower bound, this algorithm can eliminate the effect of asynchronous clock, and achieve the predicted performance in localization of mobile underwater sensor nodes.

In the future, we will explore the impact of clock skew in localization. Furthermore, we will analyze the data collision problem during the communication process.

References

[1] I. Akyildiz, D. Pompili, and T. Melodia, "Underwater acoustic sensor networks: research challenges," *Ad hoc networks*, vol. 3, no. 3, pp. 257-279, 2005.

[2] Z. Zeng, S. Fu, H. Zhang, Y. Dong, and J. Cheng, "A survey of underwater optical wireless communications," *IEEE Communications Surveys & Tutorials*, vol. 19, no. 1, pp. 204-238, 2017.

[3] Y. Noh, U. Lee, S. Lee, P. Wang, L. Vieira, J. Cui, and K. Kim, "Hydrocast: pressure routing for underwater sensor networks," *IEEE Transactions on Vehicular Technology*, vol. 65, no. 1, pp. 333-347, 2016.

[4] G. Han, H. Xu, T. Duong, T. Jiang, and T. Hara, "Localization algorithms of wireless sensor networks: a survey," *Telecommunication Systems*, vol. 52, no. 4, pp. 2419-2436. 2013

[5] L. Cheng, C. Wu, Y. Zhang, H. Wu, M. Li, and C. Maple, "A survey of localization in wireless sensor network," *International Journal of Distributed Sensor Networks*, vol. 8, no. 12, pp. 1-13, 2012.

[6] S. Wang, L. Chen, D. Gu, and H. Hu, "An optimization based moving horizon estimation with application to localization of autonomous underwater vehicles," *Robotics and Autonomous Systems*, vol. 62, no. 10, pp. 1581-1596, 2014.

[7] W. Wang and G. Xie, "Online high-precision probabilistic localization of robotic fish using visual and inertial cues," *IEEE Transactions on Industrial Electronics*, vol. 62, no. 2, pp. 1113-1124, 2015.

[8] H. Luo, K. Wu, Y. Gong, and L. Ni, "Localization for drifting restricted floating ocean sensor networks," *IEEE Transactions on Vehicular Technology*, vol. 65, no. 12, pp. 9968-9981, 2016.

[9] J. Liu, Z. Wang, Z. Peng, J. Cui, and L. Fiondella, "Suave: swarm underwater autonomous vehicle localization," in *Proceedings of the IEEE Conference on Computer Communications (INFOCOM)*, Toronto, Cannada, April 2014, 64-72.

[10] J. Yan, Z. Xu, Y. Wan, C. Chen, and X. Luo, "Consensus estimation-based target localization in underwater acoustic sensor networks," *International Journal of Robust & Nonlinear Control*, DOI: 10.1002/rnc.3198, in press, 2017.

[11] G. Isbitiren and O. Akan, "Three-dimensional underwater target tracking with acoustic sensor network," *IEEE Transactions on Vehicular Technology*, vol. 60, no. 8, pp. 3897-3906, 2011.

[12] P. Carroll, K. Mahmood, S. Zhou, H. Zhou, X. Xu, and J. Cui, "On-demand asynchronous localization for underwater sensor networks," *IEEE Transactions on Signal Processing*, vol. 62, no. 13, pp. 3337-3348, 2014.

[13] X. Cheng, H. Shu, Q. Liang, and D. Du, "Silent positioning in underwater acoustic sensor networks," *IEEE Transactions on Vehiclular Technology*, vol. 57, no. 3, pp. 1756-1766, 2008.

[14] A. Novikov and A. Bagtzoglou, "Hydrodynamic model of the lower hudson river estuarine system and its application for water quality management," *Water Resources Management*, vol. 20, no. 2, pp. 257-276, 2006.

[15] A. Caruso, F. Paparella, L. Vieira, M. Erol, "The meandering current mobility model and its impact on underwater mobile sensor networks," in *Proceedings of the IEEE Conference on Computer Communications (INFOCOM)*, Phoenix, USA, April 2008, 771-779.

[16] Z. Zhou, Z. Peng, J. Cui, Z. Shi, and A. Bagtzoglou, "Scalable localization with mobility prediction for underwater sensor networks," *IEEE Transactions on Mobile Computing*, vol. 10, no. 3, pp. 335-348, 2011.

[17] Y. Zhang, J. Liang, S. Jiang, and W. Chen, "A Localization Method for Underwater Wireless Sensor Networks Based on Mobility Prediction and Particle Swarm Optimization Algorithms," *Sensors*, vol. 16, no. 2, pp. 212-229, 2016.

[18] H. Luo, K. Wu, Y. Gong, and L. Ni, "Localization for drifting restricted floating ocean sensor networks," *IEEE Transactions on Vehicular Technology*, vol. 65, no. 12, pp. 9968-9981, 2016.

[19] G. Isbitiren and O. Akan, "Three-dimensional underwater target tracking with acoustic sensor network," *IEEE Transactions on Vehicular Technology,* vol. 60, no. 8, pp. 3897-3906, 2011.

[20] C. Rowden. Speech Processing. McGraw-Hill, 1992.

[21] A. Bagtzoglou and N. Andrei, "Chaotic behaviour and pollution dispersion characterisics in engineering tidal embayments: A numerial investigation," *Jawra Journal of the American Water Resources Association*, vol. 43, no. 1, pp. 207-219, 2007.

[22] A. Novikov and A. Bagtzoglou, "Hydrodynamic model of the lower hdson river estuarine system and its application for water quality management," *Water Resource Management*, vol. 20, no. 2, pp. 257-276, 2006.

[23] Z. Zhou, J. Cui, and S. Zhou, "Efficient localization for large-scale underwater sensor networks," *Ad Hoc Networks*, vol. 8, no. 3, pp. 267-279, 2010.

[24] S. Fortunati, F. Gini, and M. Greco, "The misspecified cramer-rao bound and its application to scatter matrix estimation in complex elliptically symmetric distributions," *IEEE Transactions on Signal Processing*, vol. 64, no. 9, pp. 2387-2399, 2016.

[25] T. Luo, W. Chen, F. Chen, F. Ji, and H. Y, "Cramer-rao bounds of source localization with distributed sensors in underwater multipath environment," in *Proceedings of MTS/IEEE Conference on Oceans,* Shanghai, China, April 2016, 1-6.

[26] S. P. Beerens, H. Ridderinkhof, J. Zimmerman. An Analytical Study of Chaotic Stirring in Tidal Areas[J]. Chaos Solitons & Fractals, 4(6):1011-1029, 1994.

[27] J. Liu, Z. Wang, J. Cui, S. Zhou, and B. Yang, "A joint time synchronization and localization design for mobile underwater sensor networks," *IEEE Transactions on Moible Computing*, vol. 15, no. 3, pp. 530-543, 2016.